Development of New generation Low-Cost Conductivity System for Crop Irrigation Monitoring

Daniel A. Basterrechea, Sandra Sendra, Sandra Viciano-Tudela, Jaime Lloret
Instituto de Investigación para la Gestión Integrada de Zonas Costeras,
Universitat Politècnica de València.
Gandía, Valencia (Spain)
Email: dabasche@epsg.upv.es, sansenco@upv.es, sandraviciano8493@gmail.com, jlloret@dcom.upv.es

***Abstract*—The development of smart cities has been boosted in recent years. This means improvements for urban agriculture. In this paper, we present a low-cost system for monitoring conductivity in the irrigation system of urban agricultural plots. For this purpose, an inductive, two-coil sensor has been developed, where one is located inside the other. For the experiment, we have used three prototypes with 40 spires for the fed part and 80 spires for the induced part, but with different pipe diameters. P1 has 20mm, P2 25 mm, and P3 32 mm. The sensors were calibrated using salt between 0 g/L and 20 g/L concentrations. We use concentration of 0 g/L, 2.5 g/L, 5 g/L, 10 g/L, 15 g/L and 20 g/L with conductivity of 0.485mS/cm, 5.53 mS/cm, 10.43 mS/cm, 20.4 mS/cm, 31.3 mS/cm, and 41.6 mS/cm. The voltage difference between the minimum and maximum concentrations in each prototype is 1.71 V for P1, 1.41 V for P2, and 0.99 V for P3. Subsequently, the verification of each prototype was performed, measuring concentrations of 7.5 g/L, 12.5 g/L, and 17 g/L, obtaining the lowest relative errors for P1 and P3 with 0.34% and 0.31% respectively.**

Keywords—Conductivity sensor; urban agriculture; irrigation monitoring.

I. INTRODUCTION

For the first time, more than half of the population lives in cities. Villages or small towns are being depopulated and more are living in cities. Due to the rural exodus, food production is becoming complicated and expensive. This situation is most relevant in developing countries, where people with limited economic resources have difficulty accessing basic foodstuffs [1].

In this situation, the smart cities (SM) concept has begun to take on great relevance [2]. SM integrates new technologies with traditional infrastructures. This synergy improves the operational and management functions of the city, increases control, and optimizes the resources of the city itself. In this context, Urban Agriculture (UA) starts to gain relevance [3]. This type of practice is carried out on relatively small plots of land and is used for the self-sufficiency of certain groups within cities. This type of agriculture reduces the carbon footprint by reducing the transport of the products obtained from the fields to the cities. Conversely, due to water resource management, many urban farmers use untreated municipal wastewater as irrigation water [4]. This can cause crop damage.

At present, the most widely used methods for controlling the quality of irrigation water are sampling and subsequent laboratory analysis. This process has several disadvantages, such as the need to have a person to take the sample, the need to have a laboratory and the waiting time for the analysis to be carried out, making it an inefficient process. One of the most relevant parameters for detecting changes in water quality is conductivity [5]. Conductivity is considered an indicator of water quality, because it displays the purity of the water or whether it contains dissolved chemicals or minerals. In this context, a high load of dissolved substances would show a high conductivity, which is harmful to the crop. Furthermore, in recent years, alternatives have emerged to monitor the quality of irrigation water. These methods are expensive or do not allow continuous monitoring in different parts of the irrigation pipes, being systems that are difficult to apply in environments such as urban plots.

In this paper, we propose the development of a low-cost system for conductivity monitoring of irrigation water used for urban agriculture. The sensor used in this system is based on the same principle as previously developed sensors [6], based on the generation of electromagnetic fields, which interact with the medium causing changes in it. The current prototype is considered progress as the design used adapts more optimally to irrigation pipes, where previous developments could not. The prototype developed has a central coil and a shallow coil around the pipe, causing minimal obstruction to the internal flow of water in the pipe.

The rest of the paper is structured as: Related works are presented in Section II. Then, the Test Bench is presented in Section III. Section IV shows the proposal performed. Then, the results are shown in Section V. Finally, the conclusion is presented in Section VI.

II. RELATED WORK

In this section, we show the different works carried out, and explain the advantages of our system compared to others.

N. A. Cloete et al. [7] proposed the design and development of a water quality monitoring system. The objective of this system is to notify the user of the real-time water quality parameters. This system is able to measure flow, temperature, pH, conductivity, and oxidation-reduction potential. They use ZigBee receiver and transmitter modules for communication. The proposed system is capable of reading physiochemical parameters, and can successfully process, transmit, and display the readings. Then, N. Vijayakumar [8], present a design and development of a low-cost system for real-time monitoring of the water quality in IoT (internet of things). This system measures different parameters like temperature, PH, turbidity, conductivity, dissolved oxygen. Moreover, they proposed the use of PI B+ model as the core controller. In the same context, F. Anthony et al [9] developed Water Sensor Network (WSN) system prototype developed for water quality monitoring in Victoria Basin (LVB). This system uses an Arduino microcontroller, water quality

 ISBN: 978-1-61208-863-1

sensors, and a wireless network connection module. The parameters that are able to measure are temperature, dissolved oxygen, pH, and electrical conductivity in real-time and disseminates the information in graphical and tabular formats to relevant stakeholders through a web-based portal and mobile phone platforms.

W. Gong et al. [10] proposed a conductivity sensor based on two flat electrodes built on a PBC board. For the measurements, they use KCI and water MQ. The sensor is suitable for marine environments. This sensor works at 334kHz obtaining significant variations in a wide range of salinity. Then, J. Zang et al [11] proposed a new four-electrode smart sensor for water conductivity measurements of aquaculture monitoring. This sensor has high precision with good stability. This system includes a temperature sensor to compensate for the water conductivity temperature dependence. The developed conductivity is appropriate for measuring conductivities between the range of 0-50 mS/cm, 0-40ºC.

Besides, J. Rocher et al [12] proposed a system for detecting illegal dumping. The proposed system is based on a conductivity sensor. This sensor is composed of two coils. One of the coils is powered by a sinus-wave and the other coil is induced. They experiment in a laboratory where the selected prototype has an 4.10 Volts between the samples 0 and 40 g/l of the table salt. Then D.A. Basterrechea et al [13] presents a test of three prototypes with different characteristics for controlling the quantity of organic fertiliser in the agricultural irrigation system. They perform the test using six samples between the 0 g/L and 20 g/L of organic fertiliser and measure their conductivity. They obtained that in prototype 1 (P1) (coil with 8 layers) the working frequency is around 100 kHz, in P2 (coil with 4 layers) around 110 kHz, and for P3 (coil with 2 layers) around 140 kHz. Finally, the results displayed that prototype three with configuration 1 is the best device to be used as a fertiliser sensor in water.

Currently, the coil designs produced are not adaptable to irrigation pipes, as these have been designed for wider spaces. Therefore, the new generation of coils developed is suitable for use in different pipe diameters.

III. TEST BENCH

In this section, we present the prototypes that have been used and the experiments that have been carried out with each group of sensors. In addition, the test bench is made up of two subsections.

A. Prototype characterization

For this experiment, we have created different prototypes for the agricultural irrigation system. These new prototypes, unlike the previous ones, can be installed in the irrigation pipes with the minimum possible interruption in the water flow. Moreover, they can be adapted to different pipe diameters. In addition, PVC of different diameters for the fed coil, such as 20 mm for P1, 25 mm for P2, and 32 mm for P3, has been used for the construction of these new prototypes. The length of the sensors used is 7.5 cm, with a thickness of 2 mm. The induced coil is placed inside the PVC pipe. For this second coil, a polyethylene (PE) pen sleeve filled with silicone has been used to create a solid core, which measures 5.3 cm. The diameter of the second reel is also 7mm. A ratio of 40 coils for the power supply (PC) on the external side and 80 coils for the induction coil (IC) on the internal side has been used.

The three prototypes developed are shown in Figure 1 where they are compared with prototype designs from previous research. The current prototype has a coil on the external side of the pipe. In comparison to the previous ones, these are suitable to be placed in the pipes directly.

B. Performance of the experiment

In order to perform our experiments, the following parameters have been selected (see Table I).

TABLE I. SELECTED PARAMETERS FOR THE EXPERIMENT.

	Parameters
Tested Frequencies	450-520 Khz
Type of water	Drinking water
Temperature	25C^{o}
NaCl concentration range	0 g/L-20 g/L

For the experiment, we started by placing two PVC elbows on each pipe to simulate real pipe conditions. In addition, we added a specific volume to each sensor. These added volumes are the ones required to cover the pipe completely. Furthermore, for P1 we used 105 mL of, 60 mL for P2, and 30 mL in P3. Once the pipe was filled, each prototype was connected one by one to the generator and oscilloscope. In this case, the supplied coil was connected to the AFG1022 generator [14] with a 3.3 V peak-to-peak supply generating a sinusoidal signal. Besides, the induced coil was connected to the TBS1104 oscilloscope.

Following the connection of the sensor, we perform a frequency scan to determine the frequency where the magnetic field generated by the sensor is most sensitive to the medium. This frequency is considered the working frequency. Once the working frequency has been obtained, we begin to take data. To do this, values are taken using 6 solutions of different NaCl concentrations. These concentrations are 0 g/L, 2.5 g/L, 5 g/L, 10 g/L, 15 g/L and 20 g/L. The conductivity is measured with a Basic-30. The conductivity values obtained are 0.485mS/cm, 5.53 mS/cm, 10.43 mS/cm, 20.4 mS/cm, 31.3 mS/cm, and 41.6 mS/cm. Triplicate values are taken and then averaged. The most stable value displayed by the oscilloscope is chosen for measurement. After taking the measurements, the calibration curve is made to determine the correlation of the values obtained with the salt concentration. Finally, verification was carried out using solutions of 7.5 g/L, 12.5 g/L, and 17 g/L, which were measured obtaining a conductivity of 15.45 mS/cm, 26.3 mS/cm, and 36.8 mS/cm.

IV. PROPOSAL

This section presents the design and test of the power circuit to generate the sinusoidal signal to power the water presence sensor.

A. ICM7555 circuit.

In order to power the different prototypes of the coil, it is required a power supply and excitation circuit to generate an alternating current similar to sinusoidal signals. To do this, a 555 series oscillator integrated circuit can be used. This circuit is configurable by using different values of resistors and capacitors. Figure 2 shows the schematic of the 555 modules in astable mode and the recommended equations for calculating the generated frequency.

 ISBN: 978-1-61208-863-1

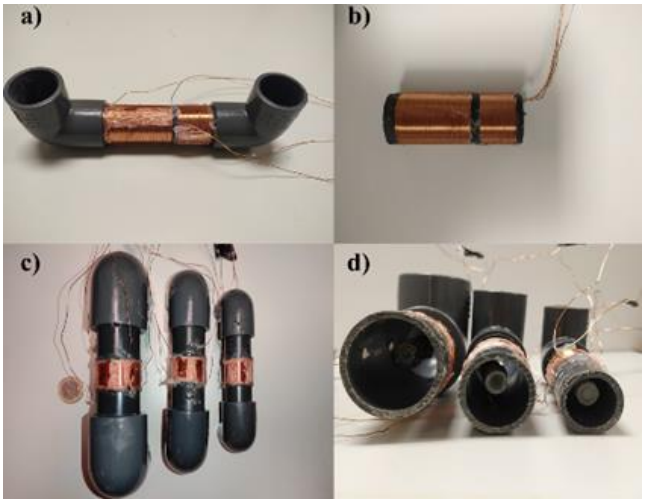

Figure 1.Design of P1, P2, and P3 (Left side) vs Older sensor (Right side).

For configuring a duty cycle of 50%, it is recommended to use the values of RA = 1 kΩ and RB = 10 kΩ. As we will see in the next section, the three prototypes we use present a working frequency between 460 kHz and 470 kHz. So, the value of C should also be determined. Using the recommended equations, we have calculated the theoretical value of C to obtain those frequencies. However, checking the actual functioning of this circuit, some differences are observed (see Table II). These differences can be due to the tolerances of all components.

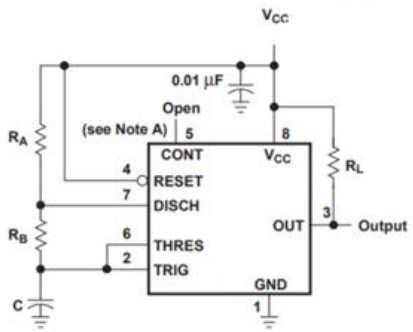

$$f \approx \frac{1.44}{(R_A + 2R_B)C} \quad (Hz)$$

$$D = \frac{R_A + R_B}{R_A + 2R_B} \cdot 100 \quad (\%)$$

Figure 2. *555 modules in astable mode and equations to determine the frequency and duty cycle.*

TABLE I. VALUES OF C FOR OBTAINING THE DESIRED FREQUENCIES

Value	C_{real}	F_{theo}	F_{real}
1	140pF	481kHz	360.6kHz
2	80pF	861kHz	468.9kHz
3	40pF	1.72MHz	505kHz

B. *Design of power circuit*

The power circuit is in charge of powering the primary coil. As we mentioned before, it is based on the ICM7555 in the astable configuration. The output voltage provided by this circuit is too low for the power of the primary coil, so, we included an NPN transistor. This component is in charge of allowing the circulating of current to the primary coil located in parallel with a resistor. The resistor placed on the collector of the NPN transistor is used to limit the current that drives through it. A diode in a flyback configuration prevents that a continuous current circulates in the coil causing the coil to become in a short-cut. The transistor will invert the sense of current through the resistor and the coil will begin to discharge until a new cycle. All these components compose the amplifier phase. In this part of the circuit, there is no AC signal. However, there is a change in the current sense, so a current is induced on the secondary coil that will help us to detect the presence of water in the pipe. Finally, it is included a Double wave rectifier bridge followed by an RC filter. Those elements are used to obtain a DC valued proportionally to the presence of water in the pipe. The circuit implemented is shown in Figure 3.

V. RESULTS

This section represents the results of the different prototypes developed and the comparison of these with prototypes made in other studies.

A. *Old prototypes*

Figure 4 shows the results obtained with the previous prototypes when applying them outside the pipe. The values obtained are homogeneous in 9.28 V at its working frequency of 210 kHz. The calibration curve reflects the fact that there is no difference between the different concentrations of salt solutions used.

B. *Current prototypes*

Figure 5 shows the frequency sweep carried out for the 3 different prototypes developed. It can be seen that the sweep frequencies performed are in a similar range for P1, P2, and P3, since the same proportion of spires has been used in both the PC and IC parts. The results obtained show that the frequencies where the voltage is higher are 480 kHz for P1 and 490 kHz for P2 and P3.

Once the frequency sweep has been carried out, measurements are taken at each of the frequencies previously displayed for different concentrations of salinity. These concentrations are in the range of 0 g/L and 20 g/L. The results obtained provide the WF of each prototype which is detailed in Table III. The WF of prototypes 1 and 2 is 470 kHz and of the P3 460 kHz. In addition, the highest voltage change is found at P1 with 1.71 V.

TABLE II. WF OF P1, P2, AND P3 WITH THEIR RESPECTIVE VOLTAGE DIFFERENCES BETWEEN THE LOWEST AND HIGHEST SALT CONCENTRATION

Prototypes	Vout (difference)	WF
1	1.71	470
2	1.41	470
3	0.99	460

 ISBN: 978-1-61208-863-1

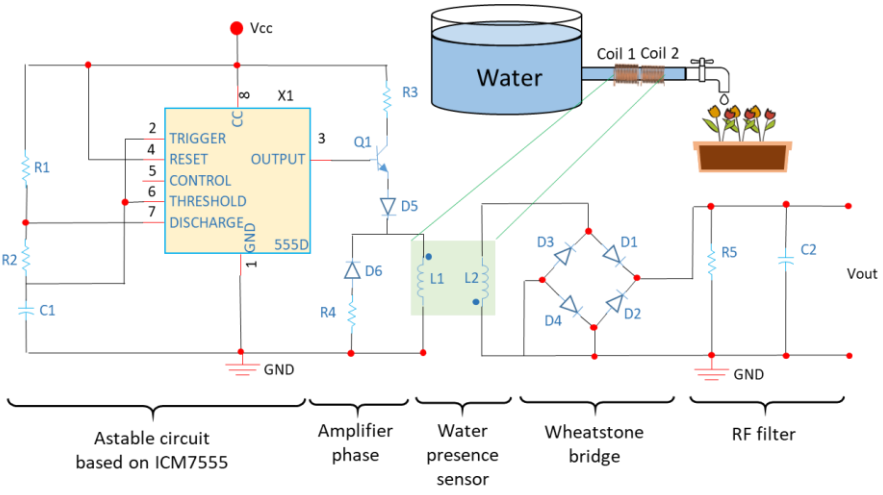

Figure 3. Power circuit schematic.

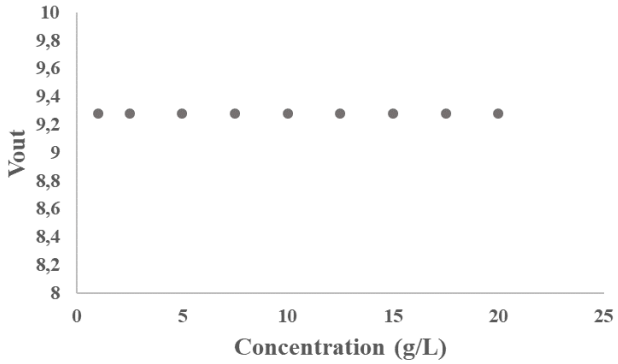

Figure. 4. Calibration of the old prototype for different NaCl concentrations.

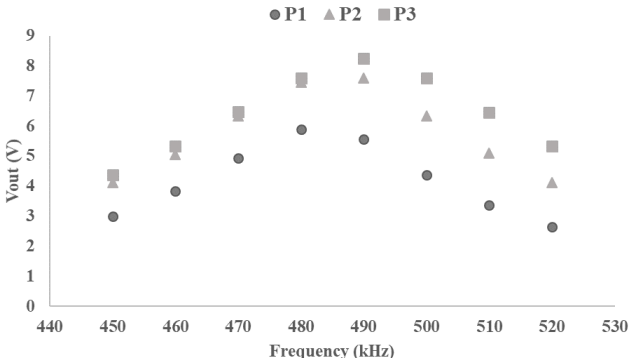

Figure 5. P1, P2, and P3 frequency sweep.

The calibration of each prototype for these frequencies was carried out once the WF was obtained, using 6 different concentrations from 0 g/L to 20 g/L every 2.5 g/L. Figure 6 represents the calibration lines for P1, P2 and P3. This represents a minimum voltage of 4.92 V and a maximum voltage of 6.63 V for P1. The change presented is about 1.71 V. The maximum changes between the measured points are located in the first 3 points, then the values stabilise. The highest variation is presented between the concentration of 0 g/L and 2.5 mg/L with 0.56 V.

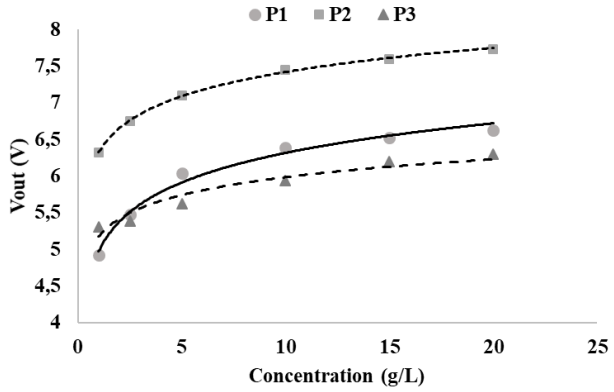

Figure 6. Calibration model of P1, P2 and P3.

Similarly, P2 shows a minimum and maximum voltage of 6.32 V and 7.73 V, with a voltage change of 1.41 V. The maximum changes between the measured points are located in the first 3 points, then the values stabilise. The highest variation is 0.42 V, presented between concentrations of 0 g/L and 2.5 mg/L.

Finally, the calibration model of P3 presented the values for the lowest concentration of 5.3 V and for the highest concentration of 6.29 V. The maximum change between these two concentrations is 0.99 V. The highest variation is presented between the concentration of 0 g/L and 2.5 mg/L with 0.24 V.

The calibration curves obtained for each of the prototypes offer a determination coefficient (R^2) whose main purpose is to predict future results or test a hypothesis. In this context, the highest R2 is found in P1 with a value of 0.9848. Then we find P2 with 0.9834 and P3 with 0.9367. The equations of each prototype are given by (1)-(3). In addition, the three prototypes present a logarithmic adjustment of the obtained values.

$$Vout = 0.5822 * \ln(Concentration(g/L)) + 4.9741 \quad (1)$$

$$Vout = 0.3960.* \ln(Concentration(g/L)) + 6.3737 \quad (2)$$

$$Vout = 0.3516 * \ln(Concentration(g/L)) + 5.1739 \quad (3)$$

C. Verification

Finally, a verification of the developed prototypes was carried out. For this purpose, 3 salt solutions of 7.5 g/L, 12.5 g/L, and 17.5 g/L were used. Table II shows the results obtained for each of the prototypes. The errors presented in the table have been obtained on an absolute value basis. Furthermore, the results show that P3 and P2 have the lowest errors, with an Absolute Error (AE) of 0.01 V and

0.02 V, and a Relative Error (RE) of 0.31 % and 0.34 % respectively. On the other hand, P2 is the one that displays the highest error with 0.13 V of AE and 1.79 % for ER.

TABLE III. VERIFICATION OF THE P1, P2, AND P3.

NaCl. (g/L)	P1		P2		P3	
	AE (Vout)	*RE (%)*	*AE (Vout)*	*RE (%)*	*AE (Vout)*	*RE (%)*
7,5	0,08	1,28	0,15	2,03	0,16	2,84
12,5	0,04	0,55	0,11	1,42	0,06	0,95
17,5	0,05	0,82	0,15	1,91	0,06	0,96
Average	0,02	0,34	0,13	1,79	0,01	0,31

In this context, we discarded P2 due to its high error compared to the others. Similarly, although P3 shows a lower error than P1, the last one is chosen as the best option for water monitoring in the irrigation system of urban agriculture. This is because P1 displays higher voltage differences between the minimum and maximum salt concentration, being 1.71 V for it versus 0.99 V for P3.

VI. CONCLUSION

Water quality monitoring in urban agriculture is of great importance to improve and optimise production from these gardens. In addition, conductivity can be classified as one of the most important parameters for detecting changes in the quality of the irrigation water used.

In this paper, we proposed a new generation low-cost system for monitoring the irrigation of urban crops. The presented sensor is optimally adapted to the irrigation pipes with minor influence on the water flow. We have determined the working frequency of the different prototypes with common salt (NaCl). The results indicate an optimal behaviour of the 3 prototypes, being the P1 the best option. This last prototype has the highest voltage difference between the minimum and maximum concentrations. In addition, the relative error is one of the smallest values of the test.

In future work, we want to improve the sensitivity of our sensor and different salts, suspended solids and pre-treated waster waters. Since it is possible to have pipes of not only PVC but also concrete and metals alloys, we would also test our system in those type of pipes and investigate the possibility of integrating them in the manufacturing of concrete coils. Finally, we will test the developed sensor in a real environment, taking measurements in a dynamic system.

ACKNOWLEDGMENT

This work has been partially supported by the European Union through the ERANETMED (Euromediterranean Cooperation through ERANET joint activities and beyond) project 41-227 SMARTWATIR.

REFERENCES

[1] F. Orsini, R. Kahane, R. Nono-Womdim and G. Gianquinto, “Urban agriculture in the developing world: a review”, *Agronomy for sustainable development* , vol. 33, no 4, pp. 695-720, May 2013, https://doi.org/10.1007/s13593-013-0143-z

[2] M. Batty et al., “Smart cities of the future”, The European Physical Journal Special Topics, vol. 214, no 1, pp. 481-518, December 2012, https://doi.org/10.1140/epjst/e2012-01703-3

[3] M. N., Poulsen, P. R. McNab, M. L. Clayton and R. A. Neff, “Sytematic review of urban agriculture and food security impacts in low-income countries”, Food Policy, vol. 55, pp. 131-146, August 2015, doi: https://doi.org/10.1016/j.foodpol.2015.07.002

[4] Food and Agriculture Organization (FAO). Water agriculture. [Online]. Available from: http://www.fao.org/fcit/upa/water-urban-agriculture/es/. [retrieved: April, 2021]

[5] T. A. Bauder, R. M. Waskom, P. L. Sutherland, and J. G. Davis. Irrigation water quality criteria. Colorado State University: doctoral thesis, 2011.

[6] J. Rocher, D. A. Basterrechea, L. Parra and J. Lloret, “New Conductivity Sensor for Monitoring the Fertigation in Smart Irrigation Systems”, International Symposium on Ambient Intelligence. Springer, Cham, June 2019, pp. 136-144, doi: https://doi.org/10.1007/978-3-030-24097-4_17.

[7] N. A. Cloete, R. Malekian and L. Nair, “Design of smart sensors for real-time water quality monitoring”, IEEE access, vol. 4, p. 3975-3990, July 2016, doi: 10.1109/ACCESS.2016.2592958.

[8] N. Vijayakumar and A. R. Ramya, “The real-time monitoring of water quality in IoT environment”, International Conference on Innovations in Information, Embedded and Communication Systems (ICIIECS), IEEE, March 2015, pp. 1-5, doi: 10.1109/ICIIECS.2015.7193080.

[9] G. Eason, B. Noble and I. N. Sneddon “On certain integrals of Lipschitz-Hankel type involving products of Bessel functions,” Phil. Trans. Roy. Soc. London, vol. A247, pp. 529–551, April 1955, doi: https://doi.org/10.1098/rsta.1955.0005.

[10] W. Gong, M. Mowlem, M. Kraft and H. Morgan, “Oceanographic sensor for in-situ temperature and conductivity monitoring”, Oceans 2008-Mts/IEEE Kobe Techno-Ocean (OTO’08), May 2008. pp. 1-6, doi: 10.1109/OCEANSKOBE.2008.4530906.

[11] J. Zhang, D. Li, C. Wang and Q. Ding, “An intelligent four-electrode conductivity sensor for aquaculture”, International Conference on Computer and Computing Technologies in Agriculture”, Springer, Berlin, Heidelberg, 2012, pp. 398-407, doi: https://doi.org/10.1007/978-3-642-36124-1_48

[12] J. Rocher, D. A. Basterrechea, M.Taha, M. Parra and , J. Lloret, “Water Conductivity Sensor based on Coils to Detect Illegal Dumpings in Smart Cities” Fourth International Conference on Fog and Mobile Edge Computing (FMEC). IEEE, June 2019. pp. 324-329, doi: 10.1109/FMEC.2019.8795341.

[13] D. A. Basterrechea, L. Parra, M. Botella-Campos, J. Lloret and P. V. Mauri, “New Sensor Based on Magnetic Fields for Monitoring the Concentration of Organic Fertilisers in Fertigation Systems” Applied Sciences, vol. 10, no 20, pp. 7222, October 2020, doi: https://doi.org/10.3390/app10207222.

[14] Farnell.[Online]. Available from: h https://es.farnell.com/tektronix/afg1022/generador-se-al-2-can-func-arb/dp/2469113_ . [retrieved:April, 2021]

 ISBN: 978-1-61208-863-1